

A quantum limit to non-equilibrium heat engine performance imposed by strong system-reservoir coupling

David Newman,^{1,2} Florian Mintert,² and Ahsan Nazir¹

¹*Department of Physics and Astronomy, The University of Manchester, Oxford Road, Manchester, M13 9PL, UK*

²*Department of Physics, Imperial College London, London, SW7 2AZ, UK*

(Dated: June 14, 2022)

We show that finite system-reservoir coupling imposes a distinct quantum limit on the performance of a non-equilibrium quantum heat engine. Even in the absence of quantum friction along the isentropic strokes, finite system-reservoir coupling induces correlations that result in the generation of coherence between the energy eigenstates of the working system. This coherence acts to hamper the engine’s power output, as well as the efficiency with which it can convert heat into useful work, and cannot be captured by a standard Born-Markov analysis of the system-reservoir interactions.

Heat engines that operate in the quantum regime have formed the basis for many theoretical studies within the past few years [1–16]. It is well understood that finite time quantum engines functioning outside the adiabatic regime are hampered by quantum friction, due to coherence that develops within the working system during the work extraction strokes [17, 18]. On the other hand, coherence can prove to be advantageous when comparing instead to the equivalent non-adiabatic stochastic (classical) engine in the limit of small action [19, 20]. Away from this limit, however, it has been argued that coherence reverts to acting as a disadvantage over the classical case [21]. With nanoscale engines no longer simply the preserve of theoretical studies, recent experimental realisations [18, 22, 23] and observations of the effects of quantum coherence in the laboratory [24] act as urgent motivation for studies of coherent engine operation.

Typical treatments of quantum engine cycles assume weak coupling, in which system-reservoir correlations are not made explicit. In the adiabatic regime, where no coherence accumulates during the work extraction strokes, this assumption also results in a reduced system state that remains diagonal in its energy eigenbasis during the heat exchange strokes. Hence, the quantum and stochastic cycles become essentially equivalent. Crucially, however, classical thermodynamic arguments for neglecting system-reservoir interaction effects are often based on the smallness of the working system surface-to-volume ratio, which breaks down at the level of individual quantum systems. Yet, the implications for non-equilibrium quantum engine performance remain to be fully explored.

Here, in contrast to previous studies that focus on work extraction, we explore the impact of system-reservoir correlations accrued as a result of finite coupling during the *heat exchange* strokes of a quantum Otto cycle. By going beyond the weak-coupling limit, but remaining adiabatic along the work extraction strokes, we show that system-reservoir correlations lead to performance losses even where quantum friction plays no role. This constitutes a distinct quantum limit to non-equilibrium engine cycles that cannot be captured by a standard weak-

coupling approach.

We consider a two-level system (TLS) which interacts separately with two heat reservoirs, at temperatures T_h and T_c with $T_h > T_c$. The Otto cycle protocol consists of four strokes labelled by eight points: $A'BB'CC'DD'A$. *Hot isochore*: at A' the TLS is coupled to the hot reservoir with which it interacts for a time τ_i to reach B . The interaction is then instantaneously set to zero at B' . *Isentropic expansion*: the self-Hamiltonian of the TLS, H_S , is tuned over a time τ such that the gap between the two energy eigenvalues is reduced to reach point C . Now, the interaction between the TLS and the cold reservoir is switched on suddenly at point C' . *Cold isochore*: the TLS interacts with the cold reservoir for a time τ_i , to reach point D . The system is then decoupled from the cold reservoir at D' . *Isentropic compression*: H_S is tuned for a time τ such that the gap between energy eigenstates is increased back to the same level as at A' , reaching point A . The cycle is completed by turning on the interaction with the hot reservoir at point A' . These strokes are repeated until a limit cycle is reached [25].

The full Hamiltonian reads

$$H(t) = H_S(t) + \sum_j (H_{R_j} + H_{I_j}), \quad (1)$$

where $H_S(t) = \epsilon(t)\sigma_z/2 + \Delta(t)\sigma_x/2$, $H_{R_j} = \sum_k \omega_{k_j} b_{k_j}^\dagger b_{k_j}$, and $H_{I_j} = -\sigma_z \sum_{k_j} f_{k_j} (b_{k_j}^\dagger + b_{k_j})$ for $j = h, c$, denoting the hot (h) and cold (c) reservoir. Here, σ_z and σ_x are the Pauli Z and X operators acting on the TLS subspace, and the TLS bias and tunneling are denoted respectively by $\epsilon(t)$ and $\Delta(t)$. The time dependence arises over the isentropic strokes when the splitting $\mu(t) = \sqrt{\epsilon(t)^2 + \Delta^2(t)}$ between the energy eigenlevels of $H_S(t)$ is tuned. We label the values of μ during the hot or cold stage of the cycle as μ_h and μ_c , respectively. Reservoir annihilation operators for excitations at frequencies ω_{k_j} are given by b_{k_j} , which satisfy bosonic commutation relations. The TLS-reservoir coupling is via H_{I_j} with strengths f_{k_j} , and the relevant interaction terms are only present during either the hot or cold isochores.

As mentioned, conventional treatments of quantum

Otto cycles invoke the weak coupling assumption, i.e. that the two interaction terms are (negligibly) small. This leads to a tractable analysis in terms of a quantum state of the TLS and reservoirs approximated to remain in tensor product form at all times. In the finite coupling regime of interest, where the interaction terms cannot be neglected, it is a more involved task to compute the state around the cycle [14–16]. In order to access this regime, we extend the reaction-coordinate (RC) formalism [26–31] from the infinite time Otto cycle considered in Ref. [29] to inherently non-equilibrium, finite time cycles. In this approach, the reservoir contributions to the interaction terms in Eq. (1) are mapped to collective modes (the RCs) such that

$$H_{I_j} = -\sigma_z \sum_{k_j} f_{k_j} (b_{k_j}^\dagger + b_{k_j}) = -\lambda_j \sigma_z (a_j^\dagger + a_j), \quad (2)$$

where a_j annihilates an excitation in the RC mode for reservoir j with natural frequency Ω_j , and $\lambda_j = (\sum_k f_{k_j}^2)^{1/2}$. The reservoir Hamiltonians become $H_{R_j} = \Omega_j a_j^\dagger a_j + \sum_{k_j} g_{k_j} (a_j^\dagger + a_j) (r_{k_j}^\dagger + r_{k_j}) + \sum_{k_j} \nu_{k_j} r_{k_j}^\dagger r_{k_j}$, while the system Hamiltonian remains unchanged. Here, r_{k_j} annihilates an excitation at frequency ν_{k_j} in a redefined residual reservoir which interacts weakly with the corresponding RC mode via couplings g_{k_j} . The full Hamiltonian thus becomes (the transformation is unitary)

$$H(t) = H_{S'}(t) + \sum_j H_{R'_j}, \quad (3)$$

where $H_{S'}(t) = \epsilon(t) \sigma_z / 2 + \Delta(t) \sigma_x / 2 - \sum_j \lambda_j \sigma_z (a_j^\dagger + a_j) + \Omega_j a_j^\dagger a_j$, and $H_{R'_j} = \sum_{k_j} g_{k_j} (a_j^\dagger + a_j) (r_{k_j}^\dagger + r_{k_j}) + \sum_{k_j} \nu_{k_j} r_{k_j}^\dagger r_{k_j}$. The RC mapping involves an enlarged view of a redefined system S' whose self-energy $H_{S'}(t)$ now additionally incorporates the self-energies of the reservoir RCs as well as the TLS-RC coupling terms. The remaining terms represent residual environments R'_j and their interactions with the corresponding RC, which may be treated as Markovian [27, 28]. This assumes a total state of product form at all times in the degrees of freedom of S' , R'_h and R'_c , but where, through the RCs, correlations between the TLS and the hot and cold reservoirs will form and indeed persist even in the limit cycle.

In the original frame and the continuum limit for bath oscillators, we characterise the TLS-reservoir interactions via spectral densities $J_j(\omega) \equiv \sum_k f_{k_j}^2 \delta(\omega - \omega_{k_j}) = \alpha \omega \omega_c / (\omega^2 + \omega_c^2)$, taken to be the same for each reservoir. Here α is the coupling strength and ω_c is a cut-off frequency. As the residual reservoirs are traced out when deriving a master equation for the enlarged system S' , to determine the RC mapping one simply needs to find the spectral density $\tilde{J}_j(\nu) \equiv \sum_k g_{k_j}^2 \delta(\nu - \nu_{k_j})$ that characterizes the coupling between S' and the residual reservoirs, as well as the parameters Ω and λ , such

that the Heisenberg equations of motion for operators in the TLS subspace are equivalent in both pictures. Imposing this results in $\Omega = 2\pi\gamma\omega_c$, $\lambda = \sqrt{\pi\alpha\Omega/2}$, and $\tilde{J}(\omega) = \omega\sqrt{\epsilon^2 + \Delta^2}/2\pi\omega_c$ [28].

The master equation governing the dynamics of S' during the j ($= h, c$) isochore is $\dot{\rho}(t) = L_j[\rho(t)]$, with $L_j[\rho(t)] \equiv -i[H_{S'_j}, \rho(t)] - [A_j, [\chi_j, \rho(t)]] + [A_j, \{\Xi_j, \rho(t)\}]$. Here, we have defined $A_j = a_j + a_j^\dagger$, the self-Hamiltonian $H_{S'_j}$ only includes interaction terms for the j RC, and the operators χ_j and Ξ_j are given by

$$\chi_j = \gamma \int_0^\infty d\tau \int_0^\infty d\omega \omega \cos(\omega\tau) \coth\left(\frac{\beta_h \omega}{2}\right) A_j(-\tau), \quad (4)$$

$$\Xi_j = \gamma \int_0^\infty d\tau \int_0^\infty d\omega \cos(\omega\tau) [H_{S'_j}, A_j(-\tau)], \quad (5)$$

where $A_j(\tau) \equiv e^{iH_{S'_j}\tau} A_j e^{-iH_{S'_j}\tau}$ [28]. The operator $\rho(t)$ represents the state of the TLS plus both reservoir RCs.

Usually, thermodynamic treatments of the Otto cycle consider thermal reservoir resources. We wish to isolate strong-coupling effects from any which may be due to coupling to heat reservoirs that are out of thermal equilibrium at the start of each isochore. To this end, we include a mechanism in our finite time cycle to ensure that any uncoupled reservoir returns to thermal equilibrium by the time it is coupled to the TLS once more. We can ensure that the uncoupled reservoir j , which has been driven out of equilibrium during the previous isochore, returns to thermal equilibrium at temperature T_j while the other reservoir and TLS interact, by adding terms to the master equation that act only on the uncoupled RC and hence do not depend on the full system plus RC eigenstructure. The uncoupled RC is a simple harmonic oscillator so we may add standard weak-coupling dissipators [32, 33]

$$L_{d_j}[\rho(t)] = \gamma_d (N_j + 1) \mathcal{L}_{a_j}[\rho(t)] + \gamma_d N_j \mathcal{L}_{a_j^\dagger}[\rho(t)], \quad (6)$$

where $\mathcal{L}_O[\rho(t)] = O\rho(t)O^\dagger - \frac{1}{2}\{O^\dagger O, \rho(t)\}$. Here, $N_j = (e^{\beta_j \Omega_j} - 1)^{-1}$ is the thermal occupation number for the uncoupled RC at inverse temperature $\beta_j = 1/T_j$. We choose the rate γ_d to ensure thermalisation occurs over a timescale such that the TLS re-couples to a thermal reservoir at the start of the subsequent isochore.

The work output of the cycle is given by the net energy change of the system across each of the isentropic strokes. For strong coupling, this also involves accounting for the energetic costs associated with turning off the interaction term at the end of the isochores; there are no coupling costs due to rethermalisation of the RCs when uncoupled. This leads to the following expression for work output [29]

$$W = \text{tr}[H_S^c \rho^C] - \text{tr}[H_S^h \rho^B] + \text{tr}[H_S^h \rho^A] - \text{tr}[H_S^c \rho^D] - \text{tr}[H_{I_h} \rho^B] - \text{tr}[H_{I_c} \rho^D], \quad (7)$$

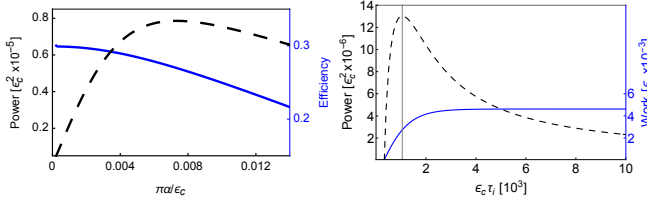


FIG. 1. Left: Power output (black dashed) and efficiency (blue) of the non-equilibrium TLS quantum Otto cycle, each as a function of coupling strength $\pi\alpha/\epsilon_c$ for $\epsilon_c\tau_i = 3000$. Right: Power (black dashed) and work (blue) output against isochore time for $\alpha = 0.01\epsilon_c/\pi$. Parameters: $\epsilon_h = 1.5\epsilon_c$, $\Delta_c = \epsilon_c$, $\Delta_h = 1.5\epsilon_c$, $\omega_c = 0.265\epsilon_c$, $\epsilon_c\beta_h = 0.95$, $\epsilon_c\beta_c = 2.5$, and 9 states in each RC.

where h and c superscripts indicate that the TLS splitting is set to μ_h and μ_c , respectively. The density operator ρ is labelled with superscripts $A - D$ indicating the various points around the cycle and as before represents the state of the enlarged S' . The energy transferred into the system during the hot isochore is given by

$$Q = \text{tr} \left[H_{S'_h}^h \rho^B \right] - \text{tr} \left[H_{S'_h}^h \rho^A \right], \quad (8)$$

and we shall term this heat. Through $H_{S'_h}$ this expression contains contributions from the TLS-hot RC interaction energy as well as a contribution from the hot RC being pulled out of equilibrium, both of which are neglected in weak-coupling treatments.

To evaluate the heat and net work output we need to compute the states ρ^{A-D} of the enlarged system S' when the engine is operating in the limit cycle. In the infinite time (equilibrium) version of the cycle, this involves taking the steady state solution of the RC master equation along each isochore, followed by unitary evolution along the isentropic strokes. For the non-equilibrium case with finite time isochores considered here, the calculation is more involved and we must numerically solve the dynamical equation of motion for the full state S' for a particular isochore time τ_i .

During the isentropic strokes we tune $\epsilon(t)$ and $\Delta(t)$ such that $(\epsilon_h, \Delta_h) \leftrightarrow (\epsilon_c, \Delta_c)$, with $[H_S(t), H_S(t')] = 0$. This ensures that the the TLS Hamiltonians at the start of the stroke, $H_S(0)$, and at the end of the stroke at time τ , $H_S(\tau)$, share a common energy eigenbasis. The TLS quantum state in this case adiabatically follows the change in splitting and no coherence develops even when the stroke is carried out in a finite time τ . We thus avoid any quantum friction along the isentropic strokes, and any variations in performance due to the generation of coherence can instead be attributed to the isochores. For the purposes of maximising power output, it is then preferable to complete this stroke quickly and we consider here the limit $\tau \rightarrow 0$.

In Fig. 1 (left) we plot the engine's power output and efficiency at finite coupling. The power output initially increases with coupling strength until a turnover is

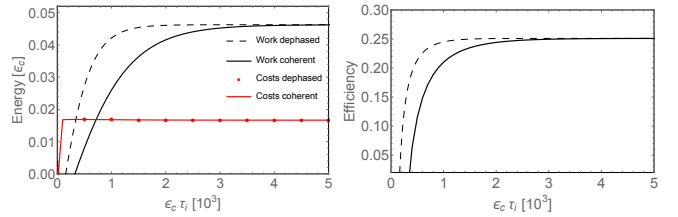


FIG. 2. Work and decoupling costs (left) and efficiency (right) plotted against isochore time $\epsilon_c\tau_i$. Solid curves represent the fully coherent engine, dotted curves depict the incoherent engine. Parameters: $\alpha = 0.01\epsilon_c/\pi$, with others as in Fig. 1.

reached as reservoir decoupling costs begin to dominate over the increase in work output. Note that we are considering here a finite isochore time, τ_i , shorter than that necessary for a stationary state to be reached along the isochore. The energy absorbed from the hot reservoir increases with coupling strength too and this leads to an engine efficiency which decreases monotonically with coupling strength. A similar finding is also reflected in the analysis of the strong coupling regime for a heat engine in Ref. [14] but there the isochores are long enough that the engine is considered to have reached arbitrarily close to equilibrium. In the present case, we show that in fact power output can be maximised before this equilibrium has been reached in Fig. 1 (right). Here we plot the work and power outputs as a function of the isochore time τ_i for an intermediate coupling strength. As the system S' approaches equilibrium, the work output saturates. Power output, however, is maximised before the working system has reached its equilibrium. If the desired metric for the engine is how much power it can produce, it is thus preferable for it to operate out of equilibrium, by choosing shorter isochore times and intermediate coupling strengths.

We now wish to explore the quantum nature of the heat engine, and specifically isolate the effects on engine performance of system-reservoir correlations accrued during the (heat exchange) isochoric strokes as a result of finite coupling with the reservoirs. These correlations manifest themselves in finite coherences in the working system state. We shall therefore make a distinction between a fully quantum version of the cycle, where system-reservoir correlations lead to quantum coherence being generated along the isochores, and one where coherence is prevented from accumulating. In this latter version of the cycle, we introduce into the master equation terms that induce pure dephasing [32, 34–37] in the energy eigenbasis of the working system, while taking care that these have no energetic contribution to the overall evaluation of work output or energy exchange with the reservoirs. To meet with these criteria, the pure dephasing terms must commute with the mapped Hamiltonian $H_{S'}$, which we diagonalise and write as $H_{S'} = \sum_n E_n |E_n\rangle \langle E_n|$. We

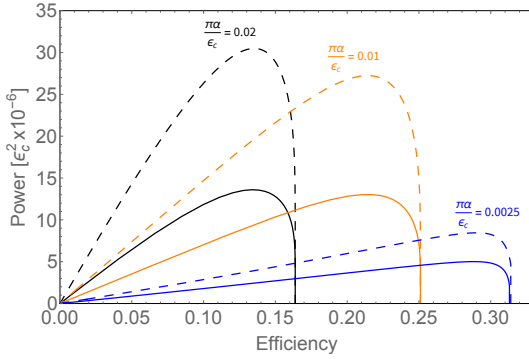


FIG. 3. Parametric plot of power output against efficiency for various coupling strengths α . Solid curves represent the fully coherent engine, dotted curves depict the incoherent engine. The parameter varied along the curves is the isochore time τ_i . Other parameters as in Fig. 1.

then construct a pure dephasing Liouvillian term as

$$L_{dep}[\rho(t)] = \gamma_{dep} \sum_n \left[[|E_n\rangle \langle E_n|, [|E_n\rangle \langle E_n|, \rho(t)]] \right]. \quad (9)$$

We are free to choose the numerical value of γ_{dep} to ensure dephasing occurs on an appropriate timescale, such that coherence is prevented from developing during the isochoric strokes of the engine. We can then compute the states of the working system at various points around the cycle as previously described, but with the addition of these terms to both isochores. We define this as the incoherent engine. We stress that these terms achieve pure dephasing in the energy eigenbasis of the enlarged TLS plus RCs (i.e. $H_{S'}$) rather than just the TLS energy eigenbasis. This is the natural choice for a system interacting strongly with an environment. Introducing pure dephasing terms into the master equation that only act on the TLS would be inappropriate since they do not commute with the unitary part of the master equation, and as such they have a non-zero energetic contribution.

We compare these two versions of the Otto cycle and analyse the effect of quantum coherence on engine performance in Fig. 2 as a function of isochore time. The solid curves depict the behaviour of the fully coherent engine, while the dotted curves represent the incoherent version of the cycle. At longer isochore times, i.e. larger τ_i , the incoherent and coherent engines converge. Here, the state of S' approaches thermal equilibrium with the relevant residual reservoir which is maintained at the hot or cold temperature. This state is then diagonal in the energy eigenbasis of S' , and so no coherence is present in either type of engine at points B or D if the isochore is long enough. For shorter times, however, this is not the case, and pure dephasing does have an appreciable effect on the engine metrics.

The dephased engine absorbs more heat along the hot isochore (not shown) but outputs a net work large enough to compensate for this, yielding a higher efficiency at

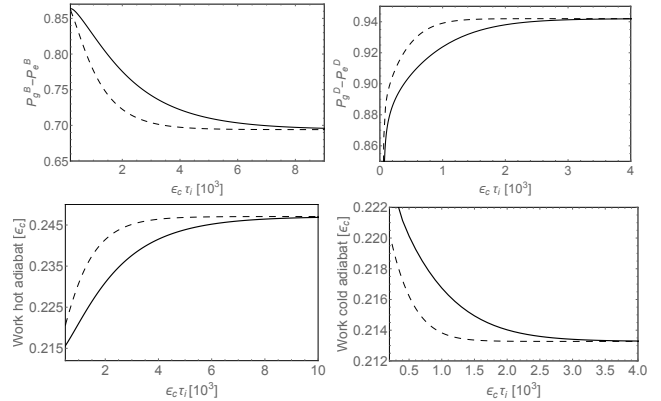


FIG. 4. TLS eigenstate population difference at point B in the cycle (top left), and at point D (top right); work extracted during the hot adiabatic stroke (bottom left) and work input during the cold adiabatic stroke (bottom right), plotted against isochore time τ_i . Solid curves represent the fully coherent engine, dotted curves depict the incoherent engine. Parameters as in Fig. 2.

short times than the fully coherent engine. Decoupling costs remain comparable. These are dominated by the RC state being driven out of equilibrium along the isochores, which is not prevented by dephasing terms. In Fig. 3 we show this improved engine performance in parametric plots of power versus efficiency when varying the isochore time, for a selection of coupling strengths. Even at weaker but finite coupling, where coherence generation is less severe, an improvement over the coherent engine can be achieved by dephasing.

In a weak coupling treatment of the Otto cycle the TLS equilibrates to a Gibbs state for long isochore times, which is diagonal in the energy eigenbasis. This is a probabilistic distribution of energy eigenstates and involves no quantum coherence. With the isentropic strokes carried out adiabatically, populations in these energy eigenstates are kept constant and no coherence in the working system state accumulates. In fact, if the isentropic strokes remain adiabatic when the cycle is treated at finite time (as we consider), then no coherence is present during the weak-coupling cycle at any time. At non-negligible system-reservoir interaction strengths, however, correlations that are generated between the TLS and the reservoir lead to quantum coherence in the energy eigenbasis at the end of the isochores. This coherence will, in general, persist during the isentropic strokes even if they are performed adiabatically. In this way, the strongly coupled TLS Otto cycle is inherently quantum in nature.

We further illustrate how dephasing in the TLS plus RC basis accelerates the process of equilibration in Fig. 4. Of crucial importance for work calculations are the differences in ground and excited state populations of the TLS in the eigenbasis of H_S [see Eq. (7)]. In Fig. 4 we show how these are affected by dephasing at point B, just before the hot adiabatic stroke begins, and at point D,

just before the cold adiabatic stroke begins. In the usual weak-coupling master equation analysis, TLS eigenbasis populations and coherences are decoupled, and so the TLS populations would be completely insensitive to pure dephasing (which for weak coupling would be properly defined relative to H_S to possess no energetic contribution). In stark contrast, for the finite coupling theory presented here, TLS populations are significantly affected by pure dephasing in the correct strong-coupling basis of H_S . Specifically, the dephased engine displays a faster approach to the steady state than the fully coherent engine. At point B there is therefore a smaller population difference (top left) at shorter τ_i and at point D a larger population difference (top right). This results in greater work extracted during the hot adiabat (bottom left) and smaller work invested during the cold adiabat (bottom right) for the dephased engine. The reason is that at point B we wish to have as much population as possible in the excited state, and therefore minimise the population difference, as this implies a higher (effective) TLS temperature. This entails that more heat has been absorbed from the hot reservoir during the hot isochore and that the subsequent hot adiabatic stroke can extract a larger amount of work. At point D, on the other hand, it is desirable to have as little population in the excited state as possible and therefore maximise the population difference. This corresponds to a lower temperature, which means that as much heat as possible has been dissipated into the cold reservoir and that on the subsequent adiabatic stroke, the work performed on the system can be kept to a minimum.

To summarise, we have shown that finite system-reservoir coupling imposes a quantum coherent limit on heat engine performance that is not captured by standard weak-coupling Born-Markov approaches. This is a distinct effect from that of quantum friction, which degrades the work extraction strokes of quantum heat engines when they are carried out in non-adiabatic conditions. Our results highlight that even when the engine is operated in an adiabatic regime for the isentropic strokes, quantum coherence enters the cycle through finite system-reservoir interactions. We thus expect our findings to be of broad relevance to practical realisations of quantum engine cycles. Schemes to mitigate this quantum disadvantage are therefore a promising avenue for further research.

We thank Luis Correa and Ronnie Kosloff for discussions. D.N. is supported by the EPSRC and the CDT in Controlled Quantum Dynamics. A.N. is supported by the EPSRC, Grant No. EP/N008154/1.

- [2] R. Kosloff, *J. Chem. Phys.* **80**, 1625 (1984).
- [3] Y. Rezek and R. Kosloff, *New J. Phys.* **8**, 83 (2006).
- [4] H. T. Quan, Y.-X. Liu, C. P. Sun, and F. Nori, *Phys. Rev. E* **76**, 031105 (2007).
- [5] N. Linden, S. Popescu, and P. Skrzypczyk, *Phys. Rev. Lett.* **105**, 130401 (2010).
- [6] L. A. Correa, J. P. Palao, G. Adesso, and D. Alonso, *Phys. Rev. E* **87**, 042131 (2013).
- [7] J. Roßnagel, O. Abah, F. Schmidt-Kaler, K. Singer, and E. Lutz, *Phys. Rev. Lett.* **112**, 030602 (2014).
- [8] R. Kosloff and A. Levy, *Annual Review of Physical Chemistry* **65**, 365 (2014).
- [9] P. Skrzypczyk, A. J. Short, and S. Popescu, *Nature Commun.* **5** (2014).
- [10] D. Gelbwaser-Klimovsky, W. Niedenzu, and G. Kurizki, *Advances In Atomic, Molecular, and Optical Physics* **64**, 329 (2015).
- [11] D. Gelbwaser-Klimovsky and A. Aspuru-Guzik, *J. Phys. Chem. Lett.* **6**, 3477 (2015).
- [12] P. P. Hofer and B. Sothmann, *Phys. Rev. B* **91**, 195406 (2015).
- [13] P. P. Hofer, J.-R. Souquet, and A. A. Clerk, *Phys. Rev. B* **93**, 041418 (2016).
- [14] M. Perarnau-Llobet, H. Wilming, A. Riera, R. Gallego, and J. Eisert, *Phys. Rev. Lett.* **120**, 120602 (2018).
- [15] P. Abiuso and V. Giovannetti, *Phys. Rev. A* **99**, 052106 (2019).
- [16] M. Wiedmann, J. T. Stockburger, and J. Ankerhold, *arXiv:1903.11368* (2019).
- [17] R. Kosloff and T. Feldmann, *Phys. Rev. E* **65**, 055102 (2002).
- [18] J. Pekola, B. Karimi, and G. Thomas, *arXiv:1812.10933* (2018).
- [19] R. Uzdin, A. Levy, and R. Kosloff, *Phys. Rev. X* **5**, 031044 (2015).
- [20] R. Uzdin, A. Levy, and R. Kosloff, *Entropy* **18** (2016).
- [21] K. Brandner, M. Bauer, and U. Seifert, *Phys. Rev. Lett.* **119**, 170602 (2017).
- [22] J. Roßnagel, S. T. Dawkins, K. N. Tolazzi, O. Abah, E. Lutz, F. Schmidt-Kaler, and K. Singer, *Science* **352**, 325 (2016).
- [23] B. Karimi and J. P. Pekola, *Phys. Rev. B* **94**, 184503 (2016).
- [24] J. Klatzow, J. N. Becker, P. M. Ledingham, C. Weinzel, K. T. Kaczmarek, D. J. Saunders, J. Nunn, I. A. Walmsley, R. Uzdin, and E. Poem, *Phys. Rev. Lett.* **122**, 110601 (2019).
- [25] R. Kosloff and Y. Rezek, *Entropy* **19(4)**, 136 (2017).
- [26] A. Nazir and G. Schaller, *The Reaction Coordinate Mapping in Quantum Thermodynamics*. In: Binder F., Correa L., Gogolin C., Anders J., Adesso G. (eds) *Thermodynamics in the Quantum Regime. Fundamental Theories of Physics*, Vol. 195 (Springer, 2019).
- [27] J. Iles-Smith, A. G. Dijkstra, N. Lambert, and A. Nazir, *J. Chem. Phys.* **144**, 044110 (2016).
- [28] J. Iles-Smith, N. Lambert, and A. Nazir, *Phys. Rev. A* **90**, 032114 (2014).
- [29] D. Newman, F. Mintert, and A. Nazir, *Phys. Rev. E* **95**, 032139 (2017).
- [30] P. Strasberg, G. Schaller, N. Lambert, and T. Brandes, *New J. Phys.* **18**, 073007 (2016).
- [31] G. Schaller, J. Cerrillo, G. Engelhardt, and P. Strasberg, *Phys. Rev. B* **97**, 195104 (2018).
- [32] H.-P. Breuer and F. Petruccione, *The theory of open*

[1] R. Alicki, *Journal of Physics A: Mathematical and General* **12**, L103 (1979).

quantum systems (Oxford University Press, Oxford, 2002).

[33] H. Carmichael, *Statistical methods in quantum optics: master equations and Fokker-Planck equations* (Springer, New York, 1999).

[34] M. A. Schlosshauer, *Decoherence and the quantum-to-classical transition* (Springer, Berlin, 2007).

[35] D. G. Tempel and A. Aspuru-Guzik, Chemical Physics **391**, 130 (2011).

[36] P. Rebentrost, M. Mohseni, I. Kassal, S. Lloyd, and A. Aspuru-Guzik, New J. Phys. **11**, 033003 (2009).

[37] T. Feldmann and R. Kosloff, Phys. Rev. E **73**, 025107 (2006).